Journal of Chromatography, 296 (1984) 3–14
Elsevier Science Publishers B.V., Amsterdam — Printed in The Netherlands

CHROMSYMP. 359

EVALUATION OF ADVANCED SILICA PACKINGS FOR THE SEPARATION OF BIOPOLYMERS BY HIGH-PERFORMANCE LIQUID CHROMATOGRAPHY

I. DESIGN AND PROPERTIES OF PARENT SILICAS

K. K. UNGER*, J. N. KINKEL, B. ANSPACH and H. GIESCHE
Institut für Anorganische Chemie und Analytische Chemie, Johannes Gutenberg-Universität, 6500 Mainz (F.R.G.)

SUMMARY

In the separation of proteins and peptides by the various modes of high-performance liquid chromatography, the nature of the substrates requires the use of microparticulate silica packings with bonded ligands of appropriate design. Agglomeration of monodisperse silica hydrosols of defined size distribution into beaded particles provides a useful method of controlling the pore size, the size distribution, the particle porosity and surface area of these packings. The particle porosity is shown to be a major factor governing the packing density and packing stability of the column. For size-exclusion chromatography of proteins, parent silicas of pore size 10 and 100 nm with a narrow pore size distribution, adequate particle porosity and low surface area should be employed for appropriate bonding, whereas reversed-phase and ion-exchange chromatography require pore sizes of 30–50 nm with specific surface areas between 50 and 100 $m^2 g^{-1}$ and particle porosities of $\leq 50\%$.

INTRODUCTION

Most current high-performance liquid chromatographic (HPLC) silica packings (either native or derivatized) were originally designed for the separation of low-molecular-weight compounds in organic and aqueous–organic eluents, and have mean pore diameters in the size range 5–15 nm, except where size-exclusion chromatography is concerned[1]. However, the analysis and isolation of biopolymers in buffered eluents by reversed-phase, ion-exchange, size-exclusion or affinity chromatography require packings of larger pore size, using covalently bonded, highly selective and stable ligands, and resulting in both high recovery and preservation of biological activity. These aspects are receiving increasing attention, but in general applicable concepts in the manufacture and derivatization of silica packings are still lacking[2,3].

In this work we investigated the mutual relationships between the surface area, porosity and pore structure of porous silica beads made by well established processes

0021-9673/84/$03.00

TABLE I

PROPERTIES OF SILICAS

Property	*Supplier and designation*			
	(1) Grace (Worms, F.R.G.) 250 Å (HPLC), 10 μm (angular), batch No. QM 02-30	*(2) E. Merck (Darmstadt, F.R.G.) LiChrospher Si 300, 5 μm (spherical), batch No. 8580*	*(3) E. Merck LiChrospher Si 500, 10 μm (spherical), batch No. WGNak 7349/M2*	*(4) DuPont (Wilmington, DE, U.S.A.) PSM 500 (spherical), batch No. 15-45 (research sample)*
Mean particle size, $d_{cc(50)}$ (μm)	10.0	5.9	7.0	6.6
Specific surface area, a_s ($m^2\ g^{-1}$)	262	259	91	19
Specific pore volume, V_p ($m^3\ kg^{-1} \cdot 10^{-3}$)	1.42	1.73	1.09	0.30
Particle porosity, P (%)	76.1	78.4	68.0	39.2
Mean pore diameter, D_{50} (nm)	38.4	32.10	53.2	59.8
Column packing density ($kg\ m^{-3} \cdot 10^3$)	0.31	0.29	0.37	0.76
Limit of packing stability, P (MPa); f_v ($ml\ min^{-1}$)	45; 6.5	50–85; 1.1	65; 8	–; –*
Loss of bed volume (%, v/v)	11.2	11.2	4.8	4.0
(at end pressure, MPa)	(48)	(90)	(92)	(92)

* Not achieved under these conditions.

and correlated these parameters with those relevant for the HPLC separation of biopolymers in the various elution modes. Based on the results obtained, the desired properties of tailor-made silicas were elucidated.

EXPERIMENTAL

Silicas

Batches of different commercial spherical and angular silicas were used, and silica beads made by spray-drying of silica sols were included (see Table I). The sols were prepared according to a procedure described by Stoeber *et al.*[4], modified in certain respects. The particle size was based on a number average and was determined by electron transmission microscopy, being equal to 264.0 ± 40.7 nm for sol A (unimodal distribution) and 234.3 and 116.5 ± 93.1 nm for sol B (bimodal distribution). The spray-dryer (an IRA-Mini-Sprühtrockenanlage HO from Labora, Weilrod-Winden, F.R.G.) was fed with 8, 14 and 20% (w/w) concentrated sols of A and 6, 10, 14 and 20% (w/w) concentrated sols of B at inlet temperatures ranging from 393 to 443°K and using an air throughput between 13 and 20 N m^3 h^{-1}.

Characterization and test procedures

From mercury porosimetry measurements the following quantities were calculated: the specific surface area according to Rootare and Prenzlow[5] using 140° as the contact angle for mercury at 298°K and 0.480 N m^{-1} for the surface tension of mercury at 298°K; the specific pore volume (v_p) measured as the volume of intruded mercury and corrected at p_{max} = 350 MPa; the pore volume distribution (pvd) from the volume *vs.* pressure plot following the Washburn equation using 140° for the contact angle at 298°K and 0.480 N m^{-1} for the surface tension of mercury at 298°K; the most frequent pore diameter ($D_{m.f.}$) measured at the maximum of the relative pvd; and the D_{50} value, measured as the pore diameter at 50% of the cumulative pvd.

Packing stability was tested by packing the silicas at p_{max} = 40 MPa and a constant flow-rate of 2–5 ml min^{-1} following the slurry method and using paraffin oil–tetrachloromethane (50:50, v/v). Columns were conditioned with water and the column back-pressure was measured as a function of the volume flow-rate, upwards to about 90 MPa and downwards by releasing the pressure.

RESULTS AND DISCUSSION

Formation of porous silica beads and the development of their pore structure

The formation of porous silica has some features in common with the process of precipitation in the production of well defined crystals. In both processes nuclei are generated as precursors, which then grow to larger particles of regular structure. With porous silica, the starting reagent (*e.g.*, an acidified solution of sodium silicate or tetraalkoxysilane) first undergoes hydrolysis, which is spontaneously followed by condensation to polysilicic acid polymers.

Nucleation occurs when the solution becomes supersaturated in the constituent species. The nuclei are assumed[6] to consist of 10–100 silica units with diameters between 1 and 2 nm. In acidic media of pH < 4 the growth of nuclei is essentially

inhibited, whereas at pH > 4 growth is promoted and larger particles (5–100 nm) are formed. The resulting silica hydrosols are composed of discrete non-porous spheres of a given size distribution. Under certain conditions silica sols are rendered stable to further growth and aggregation and can be handled up to a concentration of 50% (w/w)[7]. An alternative way to prepare silica sols is to disaggregate and disperse pyrogenic silicas (*e.g.*, Aerosil, available in graduated particle sizes between 3 and 50 nm) in water[8].

In order to prepare spherical porous particles of 1–100 μm diameter, a silica sol can be subjected to a specific process, whereby agglomeration of colloidal silica particles occurs, yielding compacts of large beads. A survey of the numerous processes in silica bead preparation (including the manufacture of beads as catalysts) was given by Iler[9]. In principle, three alternative routes can be chosen in aggregation.

(i) Gelling in a water-immiscible phase. The silica sol is dispersed into small droplets in a water-immiscible liquid. Gelling is initiated by adjusting the pH and the electrolyte concentration of the sol and/or the temperature of the dispersion liquid. During the process the liquid droplets become increasingly viscous and solidify as a coherent assembly of particles or hydrogel beads. The gelling time must be carefully related to the residence time of the droplets. The hydrogel beads are then subjected to drying, resulting in porous particles.

(ii) Agglutination. This process is based on the phenomenon of coacervation, whereby a liquid precipitate is formed by mutual coagulation of colloidal silica particles. Iler and McQueston[10] have patented such a process by which a silica–organic coacervate undergoes polymerization. The liquid coacervate precipitates from the aqueous phase as droplets, which then solidify. The organic polymer is then burned off and porous silica microspheres are obtained. The materials are marketed as chromatographic packings by DuPont (Wilmington, DE, U.S.A.) under the trade name Zorbax or PSM (*p*orous *s*ilica *m*icrospheres).

(iii) Spray-drying. A sol of a given concentration is spray-dried in air at elevated temperatures through a nozzle into a centrifugal atomizer. During spraying the liquid evaporates, leaving beads composed of compacted colloidal silica particles[11,12].

The unique composition of silica beads as an assembly of discrete non-porous spheres provides a useful basis for evaluating their surface area and their pore structure.

Porous silicas composed of a regular array of spheres[13,14]. When monodisperse colloidal silica particles are aggregated to porous bodies, the fundamental parameters characterizing the pore structure are the size (d) and the size distribution of colloidal spheres, the contact number (n) per sphere in the array and the size of the pore neck (D_n) (*i.e.* the diameter of the inscribed circle). The size of the spheres determines the specific surface area (a_s):

$$d = 6 / a_s \, d_{\text{app(He)}} \tag{1}$$

where $d_{\text{app(He)}}$ is the apparent density (helium).

It is assumed that agglomeration occurs with no substantial deposition of solid in the interparticle voids. The contact number varies between 3 and 12, *i.e.*, from

very loose to very dense agglomerates. The particle porosity (P) and the specific pore volume (v_p) vary, depending on n (see Fig. 1). D_n is calculated by

$$D_n = \frac{2.8\ v_p}{a_s} \tag{2}$$

where 2.8 is a packing coefficient averaged for n = 12, 8, 4 and 3 (ref. 13).

By combining eqns. 1 and 2 and inserting $d_{app(He)} = 2200\ kg\ m^{-3}$, one obtains

$$D_n = 1027.4\ v_p\ d \tag{3}$$

The relationships derived in eqns. 1–3 allow the calculation of the pore size as a function of the size of colloidal silica spheres and their packing density. According to eqn. 3, the size of the pore necks (D_n) equals the sphere diameter, with the specific pore volume as the proportionality factor. In a series of porous silicas with constant d and variable contact number n, the specific surface area remains the same but the particle porosity or the specific pore volume change. On the other hand, when the contact number is held constant at varying colloidal sphere diameter, the porosity has a certain value depending on n, and a_s changes according to eqn. 1.

For instance, in the PSM series the specific pore volume of PSM 60, PSM 500 and PSM 1000 is given as $0.60 \cdot 10^{-3}\ m^3\ kg^{-1}$, (ref. 15), which corresponds to a particle porosity of 56.87% and an average contact number of 5 for the colloidal spheres of the starting sols. Ramsay[12] reported v_p values between $1.40 \cdot 10^{-3}$ and 1.76

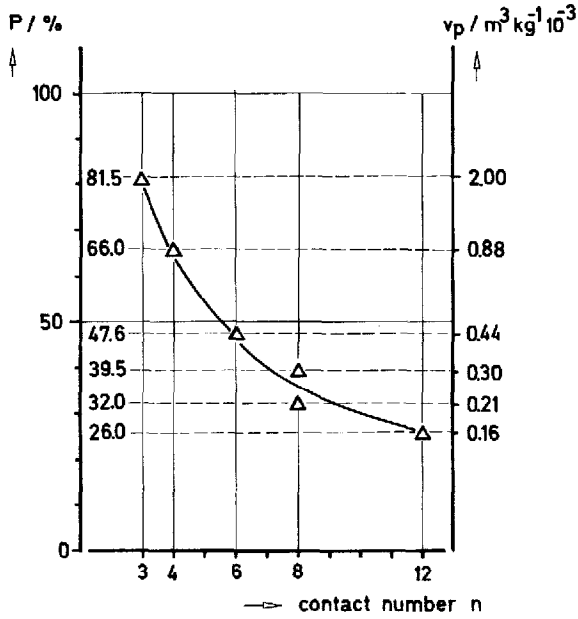

Fig. 1. Relationship between particle porosity (P) and specific pore volume (v_p) and the contact number (n) in porous silicas. P is calculated as $P = \frac{v_p}{v_p + 1/d_{app(He)}} \cdot 100\ (\%)$

$\cdot 10^{-3}$ m^3 kg^{-1} for porous silicas made by spray-drying of silica sols whose sphere diameters varied between 7 and 40 nm. Fig. 2 shows the surface of a porous silica particle composed of spheres of diameter 310 ± 20 nm with a contact number of about 8, offering a porosity of 37.55%, corresponding to a specific pore volume of $v_p = 0.267 \cdot 10^{-3}$ m^3 kg^{-1} (ref. 16).

Porous silicas composed of an irregular array of spheres. Such structures originate when monodisperse silica sols aggregate with variable contact numbers or the sols exhibit a broad unimodal or bimodal size distribution of spheres. In the latter instance the smaller particles occupy the interparticle voids between the larger particles in the aggregates. Correspondingly, the porosity is reduced compared with that of an array of monodisperse spheres.

A silica sol with a unimodal narrow sphere distribution of 264.0 ± 40.7 nm was spray-dried at 413°K and gave specific pore volumes between $0.296 \cdot 10^{-3}$ and $0.384 \cdot 10^{-3}$ m^3 kg^{-1}, depending on the starting concentration, while the specific pore volumes of porous silica beads made by a sol process with a bimodal distribution of similar mean particle size (234.3 and 116.5 ± 93.1 nm) under nearly identical conditions were $0.245 \cdot 10^{-3}$–$0.278 \cdot 10^{-3}$ m^3 kg^{-1}.

Further, there are structures known for porous silicas in which the model of aggregated spheres cannot be applied. On subjecting porous silicas to hydrothermal treatment in order to enlarge the pore size, the colloidal particles grow, whereby the

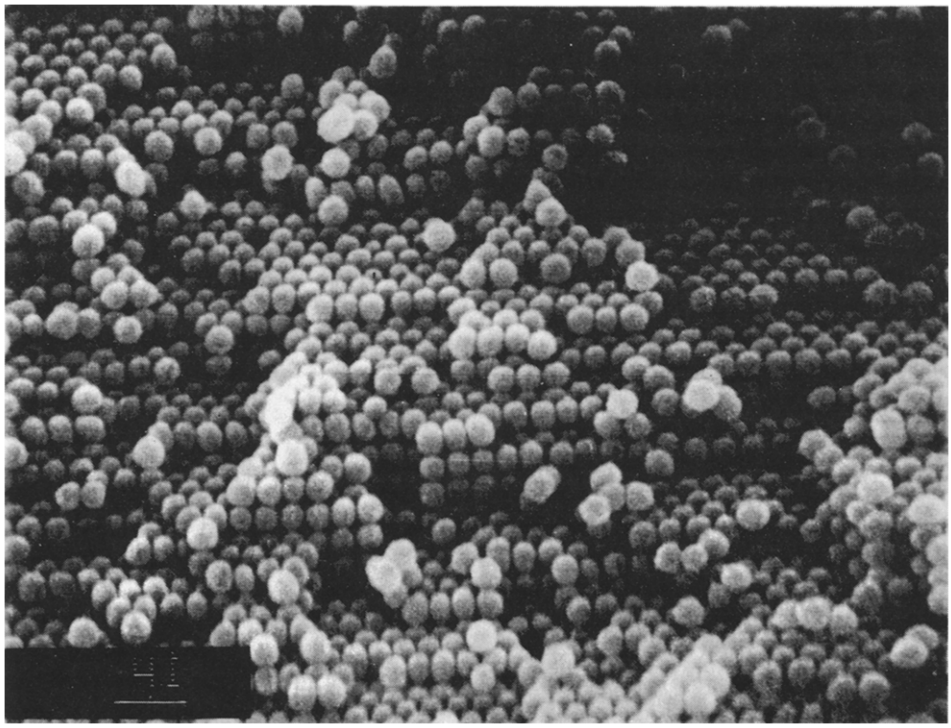

Fig. 2. Electron scanning micrograph of a particle of silica made of colloidal spheres of 310 ± 20 nm.

specific surface area drops and the mean pore diameter increases, while the specific pore volume remains constant[17]. Treatment above 513°K causes the aggregated spheres to combine to a vermicular structure, presumably owing to redeposition of amorphous or crystalline silica from the supersaturated solution during the treatment[18].

In a procedure for making silica beads by gelling polyethoxysiloxane droplets in a two-phase system, the addition of an inert solvent to the water-immiscible phase results in abnormally high specific pore volumes of the silica beads, up to $4.0 \cdot 10^{-3}$ $m^3\ kg^{-1}$ (ref. 19). Under otherwise constant conditions, v_p was found to be directly proportional to the amount of inert solvent, acting as a volume modifier, while the specific surface area remained nearly unchanged.

Properties of silica packings in relation to their use in the HPLC separation of biopolymers

Beaded vs. angular silica packings. Current trends in HPLC indicate that spherical are preferred to angular silicas, for a number of reasons. First, spherical particles permit the production of a much more homogeneous and stable column bed: while angular particles are prepared by milling and sizing of larger lumps into microparticles of narrow fractions, the mean size and size distribution of silica beads are controlled by the manufacturing process itself. Next when silicas with pores larger than 50 nm are considered for the separation of high-molecular-weight proteins, beaded silica particles offer a much higher packing stability and mechanical strength at higher flow-rates than do angular silicas of corresponding pore size.

Packing stability of silicas in HPLC. This aspect must only be considered for microparticulate silicas in the 3–15 μm size range, which are packed into columns by means of the slurry technique at pressures up to 40 MPa and high flow-rates. In order to assess the packing stability, a test procedure was applied in which columns were slurry-packed under given conditions (as indicated under Experimental) and were flushed with water and then the column back-pressure–flow-rate dependence was measured up to 90 MPa. Although such high pressures are never applied when packing and operating columns, the results may serve as a qualitative indication of the stability of silicas. The silicas subjected to the test procedure were commercial products and suitable as parent materials for biopolymer separation after appropriate modification.

The graphs of Δp *vs.* f_v (see Fig. 3) show four distinct features: (i) a linear course (identical at ascending and descending pressure and flow-rate) gives evidence that no change takes place in column bed geometry;

(ii) a pronounced step in the curve suggests that the column bed condenses under these conditions; the extent of bed compression is expressed as the ratio of the loss of bed volume after compression to the initial bed volume, in % (v/v); such a finding must be checked for reproducibility by repeating the test with virgin silica;

(iii) a hysteresis between the ascending and descending part of the Δp *vs.* f_v curve indicates that the column permeability has changed owing to the formation of a denser column bed.

(iv) an inflection of the curve towards the pressure axis is a sure indication that partial fractionation of silica particles in the column has occurred, causing a rapid drop in the flow-rate.

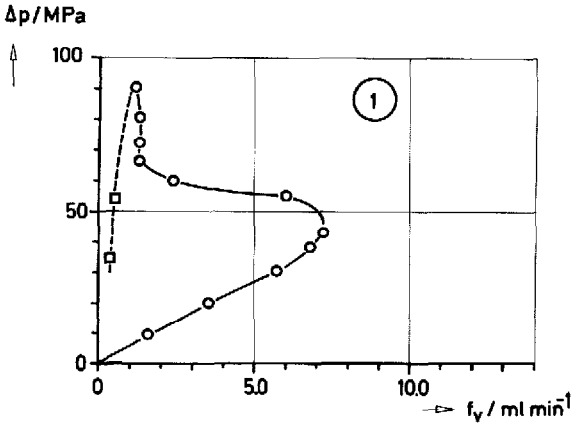
Δp/MPa
100
50
0
1
0
5.0
10.0
f_v / ml min^{-1}

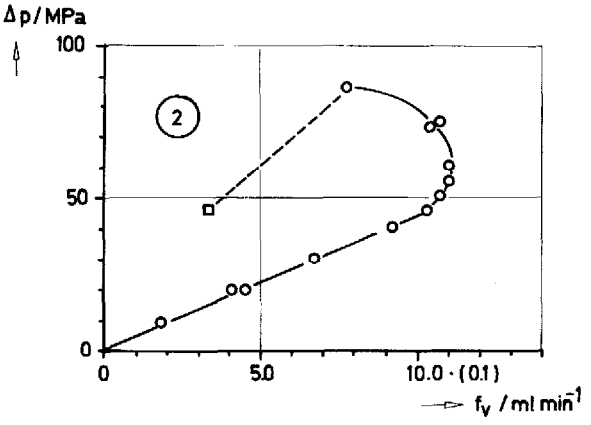
Δp/MPa
100
50
0
2
0
5.0
10.0 · (0.1)
f_v / ml min^{-1}

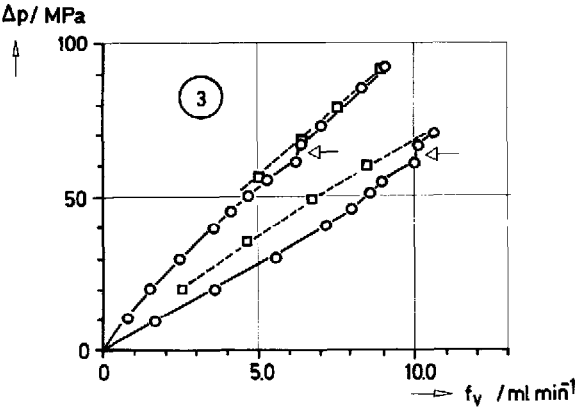
Δp/ MPa
100
50
0
3
0
5.0
10.0
f_v / ml min^{-1}

Fig. 3.

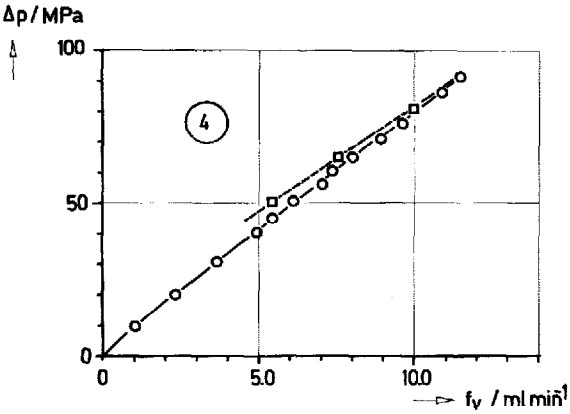

Fig. 3. Plots of column back pressure (Δ_p) *vs.* flow-rate of water for parent silicas in Table I. Column dimensions: 250 × 6 mm I.D.

The following quantities were derived (see Table I) from the graphs in Fig. 3:

(i) the limit of packing stability, *i.e.*, the pressure and corresponding flow-rate at which the material irreversibly changes its bed structure and permeability;

(ii) the ratio of the decrease in bed volume after compression at a given maximum pressure to the initial bed volume, in % (v/v).

None of the materials tested showed ideal behaviour. The only angular silica studied (No. 1) had a pore size of 25 nm and a remarkably high specific pore volume, and was crushed at 45 MPa and 6.5 ml min^{-1}, showing a volume loss of about 11%

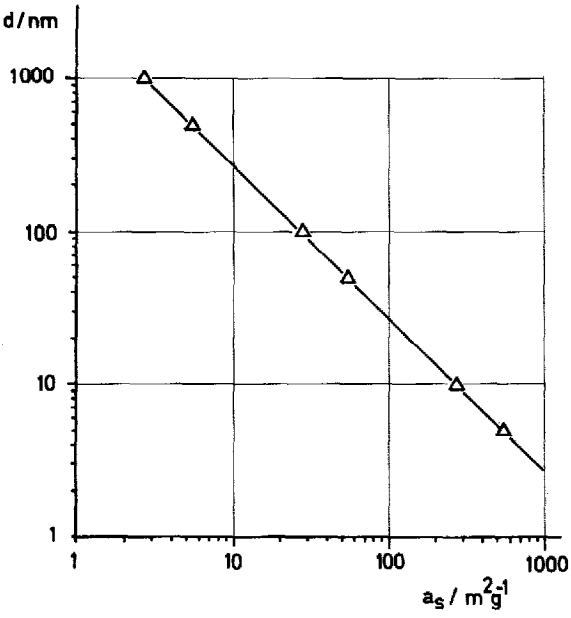

Fig. 4. Relationship between the size of colloidal spheres and the specific surface area of silica particles made by agglomeration of silica sols according to eqn. 1.

(v/v) at $p = 35$ MPa. Hence for this material pressures higher than 30 MPa should be avoided in column packing. It is worth noting that the packing density of silica 1 (measured: $0.31 \cdot 10^3$ kg m^{-3}) was about half of the value for silica 4, the latter offering a much better packing stability. The spherical silicas 2 and 3 differ in both porosity and pore size [*i.e.*, 30 and 50 nm (nominal values)]. One can see that a reduction in porosity (P) from 78.40 to 68.50 improves the packing stability by a noticeable extent and reduces the bed compaction from 11 to 5% (v/v). Silica 4 has a mean pore diameter comparable to that of silica 3, but exhibits a lower porosity ($P = 39.17\%$). Although the column is most densely packed ($0.76 \cdot 10^3$ kg m^{-3}), a change in the column bed structure occurs at 90 MPa and 11.5 ml min^{-1}.

Although the studies reported here were not exhaustive, one can nevertheless conclude that the packing stability is inversely proportional to the particle porosity and column porosity and proportional to the column packing density (see also ref. 20).

In a previous study[21] it was shown that at a constant particle porosity of about 60% the packing stability decreases with increasing pore diameter in the sequence 9.4 > 48.8 > 97.4 > 385.0 nm for spherical silicas of 10 μm particle size.

It is worth adding that the experiments carried out cannot take into account possible effects on the packing stability caused by the type and composition of the eluent.

In summary, high porosities of silica packings should be avoided where possible. In size-exclusion separations the high-porosity columns should accordingly be operated at low flow-rates, which further favours high efficiency and resolution.

Packings for size exclusion chromatography (SEC). For globular proteins the major elliptical axis falls in the range 5–50 nm whereas structural proteins, *e.g.*, collagen, have larger dimensions of up to 300 nm. In order to ensure selective permeation of the biopolymer solutes through the solid support, the mean pore size of the hydrophilic-bonded silica packing employed for this purpose should cover a range of 10–500 nm, preferably 10–100 nm. As a porous support exhibiting a narrow pore size distribution fractionates over 1.5–2 decades of molecular weight, two silica packings of pore size 10 and 100 nm are sufficient as SEC packings for globular proteins. In order to achieve a high linearity in the semilogarithmic calibration plot, the pore size distributions of both packings should not overlap if they are to be operated in tandem. SEC columns should offer a high working volume within the fractionation range. Usually this is expressed in terms of the phase ratio V_i/V_o, where V_o is the interparticle column volume and V_i the intraparticle column volume. For silicas phase ratios between 0.6 and 1.70 have been reported[22,23]. For instance, a value of 1.66 is achieved on a TSK 3000 SW column (600 × 7.5 mm I.D.)[23]. The packing material has a mean pore diameter (D_{50}) of 46.8 nm, a broad distribution, a specific surface area of 235.7 m^2 g^{-1} and a specific pore volume of $1.24 \cdot 10^{-3}$ m^3 kg^{-1} (ref. 24). Such packings, however, combine the disadvantages of limited packing stability and a high interactive surface.

To avoid second-order effects in the retention of proteins in SEC, the specific surface area of the parent silica should be low and energetically homogeneous. Fig. 4 shows the relationship between the mean sphere diameter of silica sols and the specific surface area of silica beads made from those sols. The porosity of the packings is affected only by the contact number, as illustrated in Fig. 1. The coverage with

bonded hydrophilic ligands with minimum hydrophobic character should be as dense as possible to eliminate silica matrix effects.

In conclusion, the pore size, the porosity and the specific surface area must all be considered when choosing a suitable parent silica for SEC packings.

Packings for reversed-phase (RPC) and ion-exchange chromatography (IEC). As before, the major aspect in selecting an appropriate silica for the interactive chromatography of proteins is the pore size. The bonded ligands, whether monomeric or polymeric, should be readily accessible to the proteins. Most of the commercial bonded silicas used for this purpose have pore sizes of the order of 30–50 nm, corresponding to specific surface areas of 100–50 $m^2\ g^{-1}$ for a narrow pore distribution. The actual value of the specific surface area is less important, *i.e.*, even for silicas of low surface area of 50 $m^2\ g^{-1}$ the interaction with bonded ligands is strong enough to create sufficient retention. This is a result of the multi-site attachment of proteins at the interface during retention. Also, the porosity of the packing can be as low as about 50%.

In RPC and IEC the achievement of a controlled and reproducible density of selective and stable ligands is the most decisive aspect, whereas the properties of the silica are less important, with the exception of the mean pore size.

Chemical stability of silicas. So far only the pore structure of silica in biopolymer separations has been considered. Even more important, however, are the chemical stability of bonded packings and retention effects caused by residual silanol groups.

Amorphous silica exhibits a reproducible equilibrium solubility of about 100 ppm in water at 293°K, which remains nearly constant between pH 2 and 7. Above pH 9 a steep increase in solubility occurs, caused by the formation of soluble silicates. In addition to the pH, the solubility is also dependent on the temperature, particle size and type and concentration of electrolytes[25]. One possible method of reducing the solubility of silica is to incorporate defined amounts of other metal ions (*e.g.*, aluminium) or to deposit layers of metal ions on to the surface of colloidal silica by chemisorption. Silicas made from sodium silicate solutions usually contain 500–1000 ppm of aluminium in the bulk phase[26]. The coating of colloidal silica particles with alumina has been investigated by Matijević and co-workers[27–29] and by Eulig *et al.*[30]. Silicas with an alumina-modified surface provide an increased stability over wider pH ranges and possess a stronger acid character due to an enhanced Brønsted acidity; the particles remain negatively charged down to pH 3. However, these effects have not yet been fully exploited for parent silicas and their bonded derivatives in aqueous eluents at different pH values.

In any case, even if the solubility of packings is decreased to some extent, the surface still carries charged ionic sites which give rise to ionic interactions with the biopolymers. Another possible method of eliminating these undesired effects is to bond the ligands in the form of a dense coating. Experiments indicated that polymeric layers seem to offer advantages over monomeric layers in bonding non-ionic hydrophilic ligands to silica. In the reversed-phase chromatography of peptides, however, packings are required to display graduated densities of bonded *n*-alkyl ligands, and thus the surface sites of parent silicas are still involved in the retention interactions.

CONCLUSION

It has been shown that the current technology applied in the manufacture of porous silica can be adapted to prepare beaded microparticulate silicas as parent packings for the HPLC of biopolymers. The guidelines worked out may help in optimizing the properties of these materials (*i.e.*, pore size, porosity and surface area) for each elution mode. More research is needed to improve the chemical stability of packings in both the underivatized and derivatized forms, and to improve the bonding procedures so that a reproducible density of bonded ligands may be achieved.

REFERENCES

1 R. Majors, *J. Chromatogr. Sci.*, 18 (1980) 488.
2 M. T. W. Hearn, F. E. Regnier and C. T. Wehr, *Int. Lab.*, Jan./Feb. (1983) 16.
3 M. T. W. Hearn, *Advan. Chromatogr.*, 20 (1982) 1.
4 W. Stoeber, A. Fink and E. Bohn, *J. Colloid Interface Sci.*, 26 (1968) 62.
5 H. M. Rootare and C. F. Prenzlow, *J. Phys. Chem.*, 71 (1967) 2733.
6 R. K. Iler, *The Chemistry of Silica*, Wiley-Interscience, New York, 1979, pp. 172–311.
7 R. K. Iler, *The Chemistry of Silica*, Wiley-Interscience, New York, 1979, pp. 312–461.
8 R. K. Iler, *The Chemistry of Silica*, Wiley-Interscience, New York, 1979, pp. 336–337.
9 R. K. Iler, *The Chemistry of Silica*, Wiley-Interscience, New York, 1979, pp. 526–528.
10 R. K. Iler and H. J. McQueston, *U.S. Pat.*, 3,855,172, 1974.
11 A. V. Kiselev, G. L. Kustowa, B. A. Lipkind and J. S. Nikitin, *Ger. Pat.*, 2,225,452, 1972.
12 J. D. F. Ramsay, *Ger. Pat.*, 2,647,701, 1977.
13 A. P. Karnaukhov, *Kinet. Katal.*, 12 (1971) 1025.
14 A. P. Karnaukhov, *Kinet. Katal.*, 12 (1971) 1235.
15 W. W. Yau, J. J. Kirkland and D. D. Bly, *Modern Size Exclusion Chromatography*, Wiley-Interscience, New York, 1979, p. 174.
16 S. Bukowiecki, B. Straube and K. K. Unger, *Proceedings of the Symposium on Pore Structure, Milan, April 1983*, in press.
17 A. V. Kiselev, Yu. S. Nikitin and E. B. Oganesyan, *Kolloidn. Zh.*, 31 (1969) 525.
18 A. V. Kiselev, V. M. Lukyanovich, Yu. S. Nikitin, E. B. Oganesyan and A. J. Sarakhov, *Kolloidn. Zh.*, 31 (1969) 388.
19 K. Unger and B. Scharf, *J. Colloid Interface Sci.*, 55 (1976) 377.
20 R. Ohnmacht and I. Halasz, *Chromatographia*, 14 (1981) 155.
21 K. Unger, *Porous Silica (Journal of Chromatography Library, Vol. 16)*, Elsevier, Amsterdam, 1979, pp. 174–175.
22 E. Pfankoch, K. C. Lu, F. E. Regnier and H. G. Barth, *J. Chromatogr. Sci.*, 18 (1980) 430.
23 M. E. Himmel and P. G. Squire, *Int. J. Peptide Protein Res.*, 17 (1981) 365.
24 Unpublished work; data measured by the authors by mercury porosimetry and nitrogen sorption at 77°K.
25 R. K. Iler, *The Chemistry of Silica*, Wiley-Interscience, New York, 1979, pp. 30–94.
26 R. Arras, *PhD Thesis*, Johannes Gutenberg-Universität, Mainz, 1983.
27 L. H. Allen and E. Matijevič, *J. Colloid Interface Sci.*, 33 (1970) 420.
28 L. H. Allen and E. Matijevič, *J. Colloid Interface Sci.*, 35 (1971) 66.
29 E. Matijevič, F. J. Mangravite, Jr. and E. A. Cassell, *J. Colloid Interface Sci.*, 35 (1971) 560.
30 S. Eulig, M. O. Connor and H. P. Boehm, *Z. Anorg. Allg. Chem.*, 464 (1980) 80.